Improvement of resolution and polarisation measurement precision in biomedical imaging through adaptive optics

Chao He & Martin J. Booth

Department of Engineering Science, University of Oxford, Parks Road, Oxford, OX1 3PJ, UK

chao.he@eng.ox.ac.uk; martin.booth@eng.ox.ac.uk

1, Status and challenges in tissue polarimetry

Polarimetry has many applications ranging from thin film measurement to remote sensing[1–15] One of the most important applications of polarimetric imaging, though is biomedical sample characterization, especially using polarisation microscopic/endoscopic systems[14–18]. For example, the polarimetric measurements can reveal in a label-free manner pathologies, such as cancer, that would not be otherwise detectable without staining. When all four elements of the Stokes vector of the light beam are calculated from the recorded intensity patterns, the method is known as imaging Stokes polarimetry. Likewise, imaging Mueller matrix polarimetry measures and characterizes the polarisation properties of the sample. Both methods can be used for tissue polarimetry, which has recently played an important role in biomedical characterisation and clinical diagnosis. A recent development trend has moved from full Stokes-Mueller polarimetry to partial Stokes-Mueller polarimetry, in which only a selected portion of the Stokes vector or Mueller matrix elements from the sample are measured[19]. Such an approach is adequate for specific research topics[19]. For any such vector imaging system, there are two important criteria for evaluation of imaging quality – one is the image resolution, another one is the vectorial measurement precision. In this chapter, we focus on the use of advanced adaptive optics correction methods that enhance both the imaging resolution and vector precision, hence benefiting the characterisation accuracy for biomedical samples.

The resolution of a microscope depends on the quality of its point spread function (PSF). The PSF is affected by aberrations that cause blurring and contrast reduction[20,21]. Aberrations affect all optical systems of different types and functionalities. Adaptive optics (AO) is a technology used to improve the performance of optical systems by reducing the effect of aberrations. AO uses active device such as a deformable mirror (DM) or a liquid crystal spatial light modulator (SLM), and in most cases is used to correct phase aberrations that commonly affect a wide range of imaging applications[20–22].

The AO concept was first introduced for military applications and then for astronomical telescopes[23]. AO was required in these applications to overcome the problematic effects of atmospheric turbulence, which introduced time varying aberrations into light passing through the atmosphere[23]. More recently, AO has also been deployed to microscopic imaging systems to enhance the resolution and image quality through compensation of specimen induced aberrations[20,21]. For this reason, the majority of AO applications have focussed on the phase domain.

There exists another type of aberration – polarisation aberration – which have been less well considered, but can have similar effects through blurring and reducing image contrast[19,24–34]. Moreover, they affect the measurement precision for polarisation states. These aberrations led to extra phase and polarisation distortion that can be introduced, for example, when focusing through stressed optical elements, due to Fresnel's effects at surfaces or induced via polarising effects in materials or tissues. These effects directly alter the state of polarisation (SOP) of the light field and the focal quality[19,24–34], hence degrading vectorial information analysis and the spatial resolution of optical systems that compound the effects caused by phase aberrations. Considered together, we refer to these combined polarisation and phase effects as "vectorial aberrations".

Perturbed vector states in the illumination or detection beams are greatly detrimental for polarisation sensitive microscopes, including Stokes/Mueller confocal microscopes, second/third harmonic generation microscopes and super-resolution fluorescence polarisation microscopy[19,35,36]. Such effects are vital, for example, in label-free cancer detection using Stokes/Mueller microscopes, for which the correctness of the vectorial state is essential[19]. Furthermore, incorrect polarisation disrupts the interference at the focus and hence affects the efficiency and resolution of super-resolution microscopes, for example, in the creation of the zero-intensity centre of the ring-shaped STED microscope or MINFLUX microscope

beams[37–39]; in the interference light fields of the structured illumination microscope or in 4pi microscopes[40,41]. By their nature, these systems require adaptive compensation of phase and polarisation errors to compensate for these effects that vary throughout a specimen[20,21]. We refer to these methods as "vectorial adaptive optics" or V-AO.

Similar to phase AO, V-AO requires methods for compensation of the vectorial aberrations. This requires the use of polarisation sensitive devices. Liquid crystal SLMs are good candidates to be used as vectorial correctors, as they are controllable birefringent devices[32,33]. As several parameters are required to control the vectorial state, the SLMs must be used in combination. Indeed, up to four devices are required for full vectorial compensation, as explained later in this chapter. These multiple SLMS provide the toolbox for vectorial adaptive compensation in various imaging scenarios in bio-polarimetry based sensing or imaging.

2, Vectorial aberrations and the interaction of light with specimens

2.1, Phase aberrations, polarization aberrations, and adaptive correction

Phase aberrations are usually described via a scalar phase function that varies across the beam profile[42]. The aberrations can be introduced via refractive index mismatch in specimens, misalignment of the beams through the optics, or other sources of optical path length difference. Both the state of the light beam or the aberrating action of the object are represented in a similar format. We consider the input phase field as $\Phi_{in}(r, \theta)$ and wavefront aberration induced by an object as $\Phi_{ab}(r, \theta)$ in which r and θ is the radius and azimuthal angle of the polar coordinate system of the pupil of the microscopic system. The AO correction phase is defined as $\Phi_{c}(r, \theta)$. The output phase profile $\Phi_{out}(r, \theta)$, can then be described via

(1)

It can be shown that the Zernike polynomials $Z_i(r, \theta)$ form a complete basis for representation of the aberration, if the system has circular pupils[20,21]. The output aberration function can be expressed as

(2)

where the aberration is defined over the pupil with normalised radius (for). Each of the aberration functions in Eq. 1 could similarly be represented by the coefficients of its respective Zernike series.

To illustrate the parallels between phase AO and polarisation AO, we can consider the operation of a simple focussing system with aberrations present at its input pupil. The quality of a focus is often represented by the Strehl ratio, S, which is the ratio of on axis intensity at the focal spot when aberrated, to the equivalent intensity when the system is aberration free. It is readily shown that for small phase aberrations

(3)

Where is the aberrated intensity, is the unaberrated intensity, are the coefficients of the Zernike modes and these coefficients are considered to be small. The first Zernike mode, piston (index i=1), is omitted from the summation as it represents a constant phase offset and has no effect on the measured intensity signal, so does not influence the analysis of this system. This means that there may be an arbitrary constant phase shift between the input and output phase, but this will have no effect on the system performance. In other words, the goal of the AO system is to find a correction Ψ_c that makes $\Phi_{out} - \Phi_{in}$ = constant.

This analysis is correct but incomplete, in that is assumes that the correction goal is that $\Phi_{out}(r, \theta) - \Phi_{in}(r, \theta) = \chi$, where χ represents an arbitrary constant, whereas in fact perfect correction would be achieved if $\Phi_{out}(r, \theta) - \Phi_{in}(r, \theta) = f(r, \theta)$, where the function $f(r, \theta)$ mod $2\pi = \chi$. In other words, aberrations can contain steps of an integer multiple of a wavelength and yet still provide perfect focussing.

These properties are made more obvious if we express the aberrations and system operation in terms of complex amplitudes, rather than phase, so that the Eq. 1 would be written as

(4)

where . In this formulation, each of the complex functions can be thought of as a complex multiplicative operator that operates on the function on its right. This formulation is useful, as we can use it to show parallels between the operation of phase AO and polarisation AO systems.

Polarisation aberrations have been defined by Chipman[24–29] via the Jones matrix (JM) or the Mueller matrix (MM). The polarisation aberration can be introduced in different ways, as

mentioned in previous section, and it is also linked with different physical properties, such as retardance, diattenuation and so on[24–29].

Either a JM or a MM can be used to describe the vectorial optical properties of an object. While the JM contains the information of absolute phase, it cannot represent depolarising effects of objects[19]. The MM however can represent depolarisation, but not the overall phase. Hence, the MM is used if comprehensive polarisation properties need to be considered. It is worth noting that, the SOP difference – which represents the polarisation distortion of the light beam – can also at some level represent the polarisation aberration. However, as the Stokes vector is a 4-element vector, its intrinsic dimension is lower than a multi-element matrix (with more than four free parameters), hence a full polarisation aberration is more properly described via a JM or a MM.

In this chapter we focus for simplicity on retardance-like polarisation aberrations, hence we use the JM formulism throughout the following sections. If we assume that the object introducing the polarisation aberration is a single layer of retarder, then the JM of the sample (J_s) could be written as:

(5)

where θ is the fast axis orientation with respect to the x-axis, is the retardance value, and η is the circularity[2,43–46]. We first consider the linear retarder case for which $\eta = 0$.

As the JM representation also includes the absolute phase information, we could also extract the phase aberration associated with the JM, by taking the determinant of the matrix (according to Ref[33,47]). We refer to the combined effect of an overall polarisation aberration J_{ab} with the conventional phase aberration as 'vectorial aberrations'.

When we consider a complex system that imparts various polarisation aberrations, each described through JMs: J_1, J_2, J_3, …J_n , in a particular sequence (here we assume the light beam passes in order through J_1 to J_n), the overall polarisation aberration J_{ab} can be represented via the equation:

(6)

We consider the input Jones vector field as $P_{in}(r, \theta)$ and polarisation aberration induced by an object as $J_{ab}(r, \theta)$ in which r and θ is the radius and azimuthal angle of the polar coordinate system of the pupil of the microscopic system as we used before. The AO correction

polarisation and phase is defined as $J_c(r, \theta)$. The output vectorial profile $P_{out}(r, \theta)$, can then be described via

(7)

As the multiplication of JMs is in general non-commutable, it is necessary to consider whether a system performs pre- or post-correction of the polarisation aberration. Here we describe a pre-correction AO system (Eq. (8)) and a post-correction counterpart (Eq. (9)), for which we want the $P_{out}(r, \theta)$ to features a flat wavefront and uniform polarisation state after AO system. The concept of the before- and after-correction AO systems can be illustrated via

(8)

(9)

where we take the primary matrix reciprocity problems[19] into consideration. As the matrix multiplication is in general non-commutable, the $J_c(r, \theta)$ matrices in Eq. 8 and 9 are in general different. An example of a pre-correction vectorial aberration correction AO system is illustrated in Fig 1.

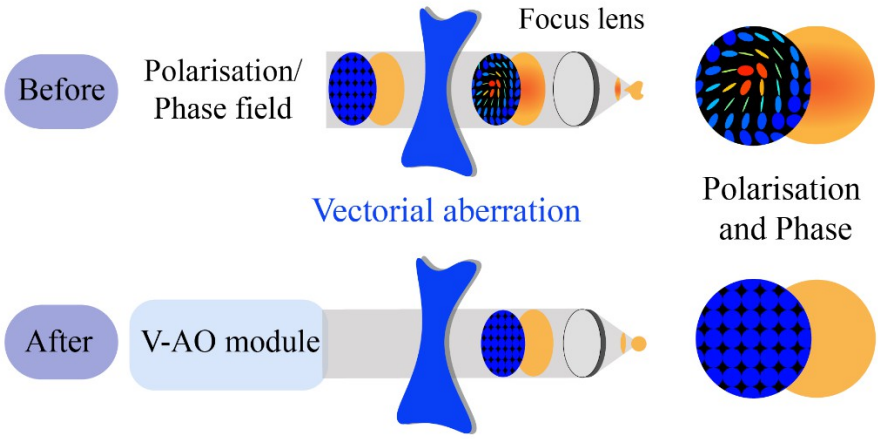

Figure 1: Vectorial aberration correction system using AO. 'Before' and 'after' illustrate the potential state of polarisation and phase correction functions. The blue and red circles in the polarisation plot represent the orientation and ellipticity/circularity of the SOP as it varies across the beam; left-hand circular SOPs are red, right-hand circular SOPs are blue, and green lines represent linear SOPs. Other shades represent different elliptical SOPs. The yellow to red colours in the phase plot represent the phase value.

A parallel can be drawn between these JM operators in the above equations, and the representation used in Eq. 4. A lossless JM can be expressed in "generator" form as[26,48,49]

(10)

where is the identity matrix and where , and represent the three Pauli spin matrices. Concisely, the first term describes polarisation independent effects on phase, which effectively means the aberration corrected by phase AO. The term represents retardation effects aligned with the and axes; retardation effects at 45° to the axes; and circular retardation effects. Although expressed here in the form of a JM, it is clear that the first term in the exponent is equivalent to the exponential phase operator of Eq. 4. Hence, the JM representation incorporates not only the polarisation states, but also the effects of the phase aberrations.

2.2, Combined effects of polarisation and phase modulation

In the context of vectorial light, normally two types of geometric phase will be involved – Rytov-Vladimirskii-Berry (RVB) phase and Pancharatnam-Berry (PB) phase[50–55]; the former is related to variation in the propagation direction of the light beam (such as when propagating in inhomogeneous media) while the latter is associated with polarisation manipulation of the light beam (such as when propagating in crystals that exhibit spatial variation of retardance across the beam profile)[50–55]. What is more, these two phases are also directly related to the process of spin-orbital interaction of light – an interaction of spin angular momentum, the intrinsic and extrinsic orbital angular momentum of light.

In this chapter, we are mainly concerned with PB-phase and retarder like systems (such as encountered in propagation through birefringent media). This extra phase shift is due to changes in SOP via the effects of the polarisation aberrations. We hence consider geometric phase as a part of the polarisation aberration, rather than a separate phenomenon. Based on this observation and the above discussion about JM, we can see that phase and polarisation aberrations are intrinsically intertwined.

3, From phase to vectorial adaptive optics for polarisation imaging

3.1, Concepts for phase, polarisation and vectorial adaptive optics

This section provides a brief summary of how AO techniques have developed from phase AO to vectorial AO for polarisation resolved imaging. Some preliminary experimental results have shown how phase AO can be used to enhance the resolution of polarisation images[56]. However, the operating mechanisms and possible applications have not yet been fully investigated. Full polarization and phase control has been previously implemented using SLMs in various configurations for generation purposes such as vector vortex beam manipulation, beam shaping and beam multiplexing[9,57,58]. However, development of the ability to control vectorial states fully to compensate vectorial beam errors has a relatively short history. Polarization and phase control for compensation of intrinsic errors in beam generation systems have been implemented[4,9,10], as has dynamic control of the full vectorial field to enable focusing through highly scattering media[59–61]. However, these works have focused mostly on complex vectorial beam generation or partial compensation of polarisation errors without full adaptive feedback correction. A systematic method for full adaptive compensation of vectorial aberrations has not yet been implemented.

Systematic adaptive polarization control to compensate externally induced polarization disturbances in pupil domain was proposed in 2019[34], where it was achieved with an SLM based correction system. The system could convert fixed SOP into arbitrary SOP[34], hence featuring the ability to perform feedback AO compensation with pre-correction of the SOP state across the pupil. That work relied upon the three fundamental components – measurement, correction, and feedback control – that are required for a full polarisation AO system. Full Stokes vector polarimetry was used to measure the polarization state across the beam profile. A dual pass SLM system was used to control the input polarization state. A strategy for feedback control was developed to enable SOP compensation from a sequence of polarimeter measurements. The methods were demonstrated on a range of specimens that perturbed the SOP of an input beam. The system restored the desired output state, even in the presence of strong polarization errors. Although the first sensor based adaptive polarization control was presented in this work, there were still certain limitations: 1) the polarisation aberration (assumed to be in the form of a spatially varying retardance) was reconstructed via prior knowledge of the aberration and the vectorial field measured by Stokes polarimetry; 2) only pupil domain correction was implemented rather than focal domain; 3) the method was

only suitable for pre-compensation of the SOP and is not readily applicable to more complex optical systems; 4) there was no phase correction.

In 2020, more general arbitrary vectorial state conversion approaches using SLMs for polarisation adaptive optics were theoretically proposed[32]. In this work, the authors also validated through JM analysis that conversion from arbitrary SOP to fixed SOP using two passes SLM is also possible, considering that in a pure retardation system the JM is fully invertible. This point is important, as it also provides the possibility of using a single SLM (with two passes through side-by-side pupils) to act as polarisation AO device for either pre- or post-correction of polarisation aberrations. Furthermore, it was shown that through using an additional SLM pass, giving three passes in total, it was possible to convert between a fixed vectorial state (polarisation and phase) to an arbitrary state or vice versa. This work also dealt with the dynamic and geometric phases arising from the polarisation effects of the SLMs. Here we briefly summarise the mathematical representation of the phase effects for a three SLM configuration; for more details one can refer to Ref[32].

The action of each of the SLMs can be described by its JM, where n is the index of the SLM, which we will refer to by the subscripts A, B and C. The output field is then determined by the input field vector via equations (see Fig. 2 for the schematic system):

(11)

where the phase is defined according to the Pancharatnam connection between the SOP before and after the SLMs. is the first eigenpolarization state of the SLM. is the SOP of the input polarisation state. The parameters and are the corresponding eigenvalues of these two states. The vector corresponds to the modulation axis of the SLM[47].

(12)

(13)

(14)

where the overall phase is represented via . The is the induced varying phase, which depends upon the SLM pixel voltage, while is the fixed phase induced along the non-modulating axis of the SLM pixel. is the retardance of the SLM at certain voltage configuration. If we

choose the orientations of SLM axes to be 0°, 45° and 0°, the corresponding eigenstates can be given by

, ,

(15)

If we have a general SOP input **,** the scalar products are given by , , and . We can therefore calculate the phases induced by each SLM pass via

(16)

The intrinsic interrelationships are elaborated in Ref[32]. Following the analysis in Ref[32], the total phase introduced by the three SLM passes equals to the sum of phase introduced individually by each pass () and the geometric phase, which is equivalent to half the area of the quadrilateral enclosed by the three passes on the Poincaré sphere (), such that

(17)

where is equal to half of the area enclosed by the path DCBA, as shown in Fig 2. In summary, the conclusion of this work showed that an extra degree of freedom is still needed to control the phase to realize full vectorial control of the beam.

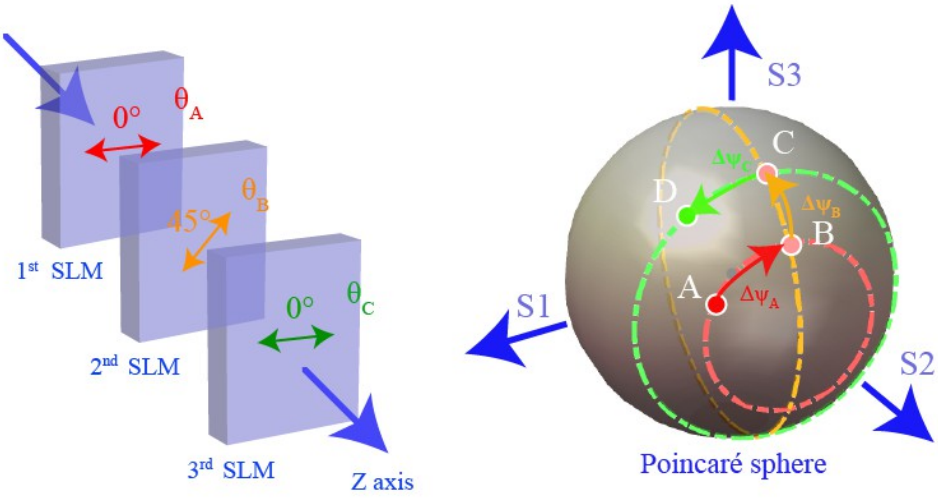

Figure 2: Schematic of the three SLM system (with modulation axis at a chosen angle θ_A, θ_B, θ_c). SOP changes on the Poincaré sphere for the three-SLM system, as the polarisation state evolves through the first SLM (A to B), the second SLM (B to C) and the third SLM (C to D)..

From the above validations we know that if one is not concerned about the phase, but only the correctness of the SOP, then with a three-pass SLM configuration, conversion between two spatially variant SOPs can be realized. While three-pass SLM configurations had been proposed and experimentally validated before, they were used for fixed SOP to arbitrary SOP and full phase control[62]. At the end of the work in Ref[32], the authors also suggested a structure with four SLMs (or three SLMs plus an alternative phase correction device, like a deformable mirror) to fully control the polarisation and phase field from any arbitrary state to another arbitrary state. This would provide a versatile vectorial field manipulation configuration with wider applications. In principle, an appropriate combination of three hypothetical retarder modulators could perform similar functionalities with less redundancy than the four-element system: e.g., one linear retarder oriented at 0°, one linear retarder at 45° and one circular retarder (or an equivalent combination).

As we have mentioned before, while there are several different SLM configurations that can manipulate the vectorial states of light, such systems are still not necessarily enough to

represent the full effects of a polarization aberration of the type that could be represented by an arbitrary unitary JM. In 2021, it was proposed to use a sequence of SLMs in a way that could reproduce the behaviour of a spatially variant waveplate with any polarisation eigenmode and arbitrary retardance distribution[33]. Hence, it provided a controllable physical system that could act as arbitrary polarisation aberration, and hence perform as the feedback correction device in a full vectorial adaptive optics system[33]. Later, a similar multi-SLM system that was equivalent to a linear phase retarder with arbitrary phase retardation was experimentally presented[63].

3.2, Vectorial adaptive optics through sensor based and sensorless methods

Traditional phase AO requires a method of phase measurement, through a wavefront sensor or indirect optimisation methods (often termed "wavefront sensorless AO" or in short "sensorless AO"), to determine the input aberration and a method of phase compensation; whereas V-AO requires the sensing and correction of the vectorial aberration. There are significant challenges in extending existing AO methods to this higher-dimensional analogue to conventional phase correction, as now we are dealing with high dimensional vector parameters rather than single scalar parameter of phase. In general, the V-AO correction can also be implemented through different methods: sensor-based and modal-sensorless; conceptual sketches of the measurement/correction process are shown in Fig 3.

Building upon previous knowledge from mathematical modelling and simulation, in 2021 the first systematic V-AO compensation technique was presented, encompassing sensor-based and sensorless approaches[64]. The work detailed sensor-based V-AO with full aberration sensing ability and a feedback correction strategy, both in the pupil and focus domains. A sensorless adaptive optics method was also implemented with a sophisticated compensation strategy. These methods were all validated via compensation of induced vectorial aberrations from various sources.

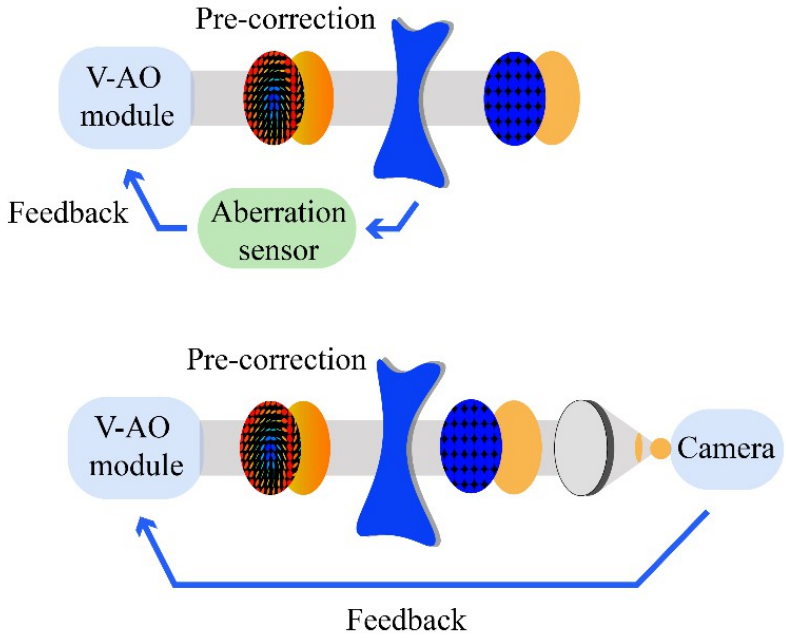

Figure 3. Illustrations of pre-correction V-AO mechanisms in the format of sensor-based (top) and sensorless (bottom) approaches.

In contrast to conventional AO, V-AO requires a method to determine the full vectorial properties, encompassing polarisation and phase, and a mechanism for control of these properties. Conventional MM polarimetry plays a role here, as the "sensor" for determination of the MM as well as the output SOP[19,30]. Note here the MM and JM provide equivalent SOP conversation information as we are dealing with non-depolarising system, and for the measurement convenience, we usually measure the MM instead of the JM as the MM can be determined solely from intensity-based measurements. Sensorless V-AO methods can also be employed, for example allowing model-based optimisation of focal quality through adjustment of polarisation and phase states. Sensorless AO is useful, as it does not require any additional sensor and can permit efficient optimisation of vectorial correction through sequence of images. Such methods are widely used in phase AO, where modes such as Zernike polynomials are applied and optimised. The principle can be extended to vectorial AO, as both polarisation and phase aberrations affect image quality. An easy to explain example is when there is prior knowledge of, e.g., the retardance axis, but unknown retardance magnitude. Appropriate vectorial aberration modes can be applied to enable image optimisation. Correction of more complex vectorial aberrations with more unknown parameters could be implemented with more complex aberration modes.

More description of the methods and their properties, with demonstrations of the improvement of both vector field and focus after correction of commonplace vectorial aberrations, can be found in Ref[64].

4, Prospects for vectorial adaptive optics

4.1, Vectorial image enhancement: label-based and label-free

Vectorial adaptive optics has not yet been applied into areas of vectorial imaging, which includes fluorescence-based approaches as well as the label-free polarisation imaging methods.

Advanced fluorescence polarisation microscopy (FPM)[65–68], which harnesses vectorial information about dipole emitters, has recently been attracting scientific attention. Vectorial information is encoded in the SOP of the emitted light, which is normally linearly polarised. The polarimetric detection of dipole orientation and subsequent analysis plays an important role in biomedical sample analysis. For instance, the dipole behaviours that are revealed via FPM techniques can be used to study cytoskeleton components such as actin, myosin, and microtubules, as well as septin. They have also been used to analyse the nuclear pore complex subcomplexes and their relative orientations[69–73]. Recent advances also include fluorescent dipoles super-resolution imaging via polarised illumination[74,75]. As any of these high resolution microscopes can suffer from polarisation aberrations, these areas have potential to be benefit from V-AO techniques.

For label-free biomedical polarimetry, cancer detection is an important application[14,15,17–19,30]. Recently, such polarimetric techniques have supported the diagnosis of various cancerous tissues, such as human skin cancer, colon cancer, liver cancer and breast cancer[19]. Polarimetric data has been used to analyse the fibrosis process among different stages of cancer development, which can be implemented via evaluation of polarimetric parameters such as retardance value[19]. Similarly, the fast axis orientation of the retardance is also used to describe the distribution of features in the fibrous regions, which has also assisted pathological diagnosis[19]. In these applications, any polarisation aberration within the measurement process, such as intrinsic polarisation aberrations from the high numerical aperture lenses[76], would also significantly affect the resolution, as well as the correctness of those quantitative vectorial metrics that are used for clinical diagnoses.

4.2, Compensation of other vectorial aberrations: diattenuator and depolariser

There are many other possible polarisation perturbations besides the pure retardance aberrations that have mostly been discussed in this chapter. These other types of polarisation perturbations include diattenuation and depolarisation. In this section we also give a brief explanation of strategies for their estimation and compensation.

For diattenuation-based polarisation aberrations, which arise due to intrinsic anisotropic absorption properties, some intensity, and hence information, must be lost from the original light beam[19]. It is not possible to retrieve this lost power through existing AO methods. Post acquisition image processing can be taken into consideration as a partial solution. However, diattenuation can cause a change in the SOP, which it is possible to compensate using the V-AO methods proposed before. For small diattenuation aberrations, SOP errors can generally be fully compensated using V-AO. On the other hand, if there exists a large diattenuation aberration, the consequences could be more serious. If the extinction ratio of the diattenuation is very high (in the extreme case, infinite), then any incident SOP (possibly pre-compensated with V-AO) will be converted into a fixed SOP (with varying intensity) after the diattenuation aberration. Hence, any V-AO pre-compensation would have limited use. Similar problems would occur in systems where post-compensation is required.

Depolarisation is a very important vectorial parameter that can affect various techniques and their corresponding applications[19]. For example, in biomedical applications, depolarisation can be used as an indicator to monitor the condition of muscle *in vivo* or for differentiating normal/cancerous tissue *ex vivo*[77]; it is also an important parameter to assess the performance in the waveguide chips for quantum computers[78].

There exist two possible parts of the distortion introduced by depolarisation – SOP distortion and degrees of polarisation (DOP) distortion. The former can be possibly corrected via the V-AO tools that were explained earlier in this chapter, while the DOP errors might be corrected via new devices featuring polarizance properties (the ability to enhance the DOP). In conclusion, these cutting-edge V-AO techniques would not only provide possibilities for higher image resolution, but also improved vectorial information measurement precision in biomedical imaging and clinical applications.

Reference:

1. Oldenbourg, R. A new view on polarization microscopy. *Nature* **381**, 811–812 (1996).
2. Chipman, R. A., Lam, W.-S. T. & Young, G. *Polarized light and optical systems*. (CRC press, 2018).
3. Cloude, S. *Polarisation: applications in remote sensing*. (OUP Oxford, 2009).
4. Rubinsztein-Dunlop, H. *et al.* Roadmap on structured light. *J. Opt.* **19**, 13001 (2016).
5. Radwell, N., Hawley, R. D., Götte, J. B. & Franke-Arnold, S. Achromatic vector vortex beams from a glass cone. *Nat. Commun.* **7**, 1–6 (2016).
6. Ndagano, B. *et al.* Characterizing quantum channels with non-separable states of classical light. *Nat. Phys.* **13**, 397–402 (2017).
7. Rubin, N. A. *et al.* Matrix Fourier optics enables a compact full-Stokes polarization camera. *Science (80-.).* **365**, eaax1839 (2019).
8. Curcio, V., Alemán-Castañeda, L. A., Brown, T. G., Brasselet, S. & Alonso, M. A. Birefringent Fourier filtering for single molecule coordinate and height super-resolution imaging with dithering and orientation. *Nat. Commun.* **11**, 1–13 (2020).
9. Rosales-Guzmán, C., Ndagano, B. & Forbes, A. A review of complex vector light fields and their applications. *J. Opt.* **20**, 123001 (2018).
10. Wang, J., Castellucci, F. & Franke-Arnold, S. Vectorial light–matter interaction: Exploring spatially structured complex light fields. *AVS Quantum Sci.* **2**, 31702 (2020).
11. Azzam, R. M. A. Stokes-vector and Mueller-matrix polarimetry. *JOSA A* **33**, 1396–1408 (2016).
12. Tyo, J. S., Goldstein, D. L., Chenault, D. B. & Shaw, J. A. Review of passive imaging polarimetry for remote sensing applications. *Appl. Opt.* **45**, 5453–5469 (2006).
13. Novikova, T., Meglinski, I., Ramella-Roman, J. C. & Tuchin, V. V. Special section guest editorial: polarized light for biomedical applications. *J. Biomed. Opt.* **21**, (2016).
14. Qi, J. & Elson, D. S. Mueller polarimetric imaging for surgical and diagnostic applications: a review. *J Biophotonics* **10**, 950–982 (2017).
15. He, H. *et al.* Mueller Matrix Polarimetry-An Emerging New Tool for Characterizing the Microstructural Feature of Complex Biological Specimen. *J. Light. Technol.* **37**, 2534–2548 (2019).
16. Ghosh, N. & Vitkin, A. I. Tissue polarimetry: concepts, challenges, applications, and outlook. *J. Biomed. Opt.* **16**, 110801 (2011).
17. Tuchin, V. V. Polarized light interaction with tissues. *J. Biomed. Opt* **21**, 71114 (2016).

18. Ramella-Roman, J. C., Saytashev, I. & Piccini, M. A review of polarization-based imaging technologies for clinical and preclinical applications. *J. Opt* **22**, (2020).

19. He, C. *et al.* Polarisation optics for biomedical and clinical applications: a review. *Light Sci. Appl.* **10**, 194 (2021).

20. Booth, M. J. Adaptive optical microscopy: the ongoing quest for a perfect image. *Light Sci. Appl.* **3**, e165–e165 (2014).

21. Ji, N. Adaptive optical fluorescence microscopy. *Nat. Methods* **14**, 374–380 (2017).

22. Do, T. *et al.* Relativistic redshift of the star S0-2 orbiting the Galactic Center supermassive black hole. *Science (80-.).* **365**, 664–668 (2019).

23. Beckers, J. M. Adaptive optics for astronomy: principles, performance, and applications. *Annu. Rev. Astron. Astrophys.* **31**, 13–62 (1993).

24. Chipman, R. A. & Chipman, L. J. Polarization aberration diagrams. *Opt. Eng.* **28**, 100–106 (1989).

25. Breckinridge, J. B., Lam, W. S. T. & Chipman, R. A. Polarization aberrations in astronomical telescopes: the point spread function. *Publ. Astron. Soc. Pacific* **127**, 445 (2015).

26. McGuire, J. P. & Chipman, R. A. Polarization aberrations. 1. Rotationally symmetric optical systems. *Appl. Opt.* **33**, 5080–5100 (1994).

27. McGuire, J. P. & Chipman, R. A. Polarization aberrations. 2. Tilted and decentered optical systems. *Appl. Opt.* **33**, 5101–5107 (1994).

28. Chipman, R. A. Polarization Analysis Of Optical Systems. *Opt. Eng.* **28**, 90–99 (1989).

29. McGuire, J. P. & Chipman, R. A. Diffraction image formation in optical systems with polarization aberrations. I: Formulation and example. *JOSA A* **7**, 1614–1626 (1990).

30. He, C. *et al.* Revealing complex optical phenomena through vectorial metrics. *Adv. Photonics* **4**, 26001 (2022).

31. He, C., Hu, Q., Dai, Y. & Booth, M. J. Vectorial adaptive optics - correction of polarization and phase. in *Imaging and Applied Optics Congress* OF2B.5 (Optical Society of America, 2020). doi:10.1364/AOMS.2020.OF2B.5.

32. Hu, Q., Dai, Y., He, C. & Booth, M. J. Arbitrary vectorial state conversion using liquid crystal spatial light modulators. *Opt. Commun.* **459**, 125028 (2020).

33. Hu, Q., He, C. & Booth, M. J. Arbitrary complex retarders using a sequence of spatial light modulators as the basis for adaptive polarisation compensation. *J. Opt.* **23**, 65602 (2021).

34. Dai, Y. *et al.* Active compensation of extrinsic polarization errors using adaptive optics. *Opt. Express* **27**, 35797–35810 (2019).

35. Morizet, J. *et al.* High-speed polarization-resolved third-harmonic microscopy. *Optica* **6**, 385–388 (2019).

36. Chen, L. *et al.* Advances of super-resolution fluorescence polarization microscopy and its applications in life sciences. *Comput. Struct. Biotechnol. J.* **18**, 2209–2216 (2020).

37. Hao, X. *et al.* Three-dimensional adaptive optical nanoscopy for thick specimen imaging at sub-50-nm resolution. *Nat. Methods* **18**, 688–693 (2021).

38. Hao, X., Kuang, C., Wang, T. & Liu, X. Effects of polarization on the de-excitation dark focal spot in STED microscopy. *J. Opt.* **12**, 115707 (2010).

39. Gwosch, K. C. *et al.* MINFLUX nanoscopy delivers 3D multicolor nanometer resolution in cells. *Nat. Methods* **17**, 217–224 (2020).

40. Wang, J. *et al.* Implementation of a 4Pi-SMS super-resolution microscope. *Nat. Protoc.* **16**, 677–727 (2021).

41. Žurauskas, M. *et al.* IsoSense: frequency enhanced sensorless adaptive optics through structured illumination. *Optica* **6**, 370–379 (2019).

42. Booth, M. J. Adaptive optics in microscopy. *PHIL TRANS R SOC A* **365**, 2829–2843 (2007).

43. Ronchi, V. *The nature of light : an historical survey*. (Heinemann, 1970).

44. Goldstein, D. H. *Polarized light*. (CRC press, 2017).

45. Huard, S. *Polarization of light*. (1997).

46. Gil, J. J. & Ossikovski, R. *Polarized light and the Mueller matrix approach*. (CRC press, 2022).

47. Gutiérrez-Vega, J. C. Pancharatnam–Berry phase of optical systems. *Opt. Lett.* **36**, 1143–1145 (2011).

48. Jones, R. C. A new calculus for the treatment of optical systems. VII. Properties of the N-matrices. *Josa* **38**, 671–685 (1948).

49. Carl, M. Influence of polarization aberrations on point images. *JOSA A* **34**, 967–974 (2017).

50. Ling, X. *et al.* Giant photonic spin Hall effect in momentum space in a structured metamaterial with spatially varying birefringence. *Light Sci. Appl.* **4**, e290–e290 (2015).

51. Ling, X. *et al.* Recent advances in the spin Hall effect of light. *Reports Prog. Phys.* **80**, 66401 (2017).

52. Ling, X., Zhou, X., Shu, W., Luo, H. & Wen, S. Realization of tunable photonic spin Hall effect by tailoring the Pancharatnam-Berry phase. *Sci. Rep.* **4**, 1–5 (2014).

53. Bliokh, K. Y., Aiello, A. & Alonso, M. A. Spin-orbit interactions of light in isotropic media. *Angular Momentum Light* 174–245 (2012).

54. Liberman, V. S. & Zel'dovich, B. Y. Spin-orbit interaction of a photon in an inhomogeneous medium. *Phys. Rev. A* **46**, 5199 (1992).

55. Cardano, F. & Marrucci, L. Spin–orbit photonics. *Nat. Photonics* **9**, 776–778 (2015).

56. Song, H., Zhao, Y., Qi, X., Chui, Y. T. & Burns, S. A. Stokes vector analysis of adaptive optics images of the retina. *Opt. Lett.* **33**, 137–139 (2008).

57. Zhan, Q. Cylindrical vector beams: from mathematical concepts to applications. *Adv. Opt. Photonics* **1**, 1–57 (2009).

58. Forbes, A., de Oliveira, M. & Dennis, M. R. Structured light. *Nat. Photonics* **15**, 253–262 (2021).

59. Park, J., Park, J.-H., Yu, H. & Park, Y. Focusing through turbid media by polarization modulation. *Opt. Lett.* **40**, 1667–1670 (2015).

60. Yang, J., Shen, Y., Liu, Y., Hemphill, A. S. & Wang, L. V. Focusing light through scattering media by polarization modulation based generalized digital optical phase conjugation. *Appl. Phys. Lett.* **111**, 201108 (2017).

61. Yu, P., Zhao, Q., Hu, X., Li, Y. & Gong, L. Tailoring arbitrary polarization states of light through scattering media. *Appl. Phys. Lett.* **113**, 121102 (2018).

62. Peña, A. & Andersen, M. F. Complete polarization and phase control with a single spatial light modulator for the generation of complex light fields. *Laser Phys.* **28**, 76201 (2018).

63. Yu, C.-J. & Chou, C.-X. Electrically rotated retarder/diattenuator system for application to a variety of polarization elements. *Opt. Commun.* **508**, 127809 (2022).

64. He, C., Antonello, J. & Booth, M. J. Vectorial adaptive optics. (2021).

65. Soni, J. *et al.* Quantitative fluorescence and elastic scattering tissue polarimetry using an Eigenvalue calibrated spectroscopic Mueller matrix system. *Opt. Express* **21**, 15475–15489 (2013).

66. Jagtap, J. *et al.* Quantitative Mueller matrix fluorescence spectroscopy for precancer detection. *Opt. Lett.* **39**, 243–246 (2014).

67. Hafi, N. *et al.* Fluorescence nanoscopy by polarization modulation and polarization angle narrowing. *Nat. Methods* **11**, 579–584 (2014).

68. Cruz, C. A. V. *et al.* Quantitative nanoscale imaging of orientational order in biological filaments by polarized superresolution microscopy. *Proc. Natl. Acad. Sci.* **113**, E820–E828 (2016).

69. Sase, I., Miyata, H., Ishiwata, S. & Kinosita, K. Axial rotation of sliding actin filaments revealed by single-fluorophore imaging. *Proc. Natl. Acad. Sci.* **94**, 5646–5650 (1997).

70. Forkey, J. N., Quinlan, M. E., Alexander Shaw, M., Corrie, J. E. T. & Goldman, Y. E. Three-dimensional structural dynamics of myosin V by single-molecule fluorescence polarization. *Nature* **422**, 399–404 (2003).

71. Sosa, H., Peterman, E. J. G., Moerner, W. E. & Goldstein, L. S. B. ADP-induced rocking of the kinesin motor domain revealed by single-molecule fluorescence polarization microscopy. *Nat. Struct. Biol.* **8**, 540–544 (2001).

72. DeMay, B. S. *et al.* Septin filaments exhibit a dynamic, paired organization that is conserved from yeast to mammals. *J. Cell Biol.* **193**, 1065–1081 (2011).

73. DeMay, B. S., Noda, N., Gladfelter, A. S. & Oldenbourg, R. Rapid and quantitative imaging of excitation polarized fluorescence reveals ordered septin dynamics in live yeast. *Biophys. J.* **101**, 985–994 (2011).

74. Axelrod, D. Carbocyanine dye orientation in red cell membrane studied by microscopic fluorescence polarization. *Biophys. J.* **26**, 557–573 (1979).

75. Schütz, G. J., Schindler, H. & Schmidt, T. Imaging single-molecule dichroism. *Opt. Lett.* **22**, 651–653 (1997).

76. Shen, Y. *et al.* Polarization Aberrations in High-Numerical-Aperture Lens Systems and Their Effects on Vectorial-Information Sensing. *Remote Sens.* **14**, 1932 (2022).

77. Du, E. *et al.* Mueller matrix polarimetry for differentiating characteristic features of cancerous tissues. *J. Biomed. Opt.* **19**, 76013 (2014).

78. Cai, Z. Multi-exponential error extrapolation and combining error mitigation techniques for nisq applications. *npj Quantum Inf.* **7**, 1–12 (2021).